Article ID: 1000-324X(2023)12-1475-08 **DOI:** 10.15541/jim20230059

Crystal Growth and Structural, Optical, and Visible Fluorescence Traits of Dy^{3+}-doped $SrGdGa_3O_7$ Crystal

WANG Haidong[1,2,3], WANG Yan[1,3], ZHU Zhaojie[1,3], LI Jianfu[1,3], LAKSHMINARAYANA Gandham[4], TU Chaoyang[1,3]

(1. Fujian Institute of Research on the Structure of Matter, Chinese Academy of Sciences, Fuzhou 350002, China; 2. University of Chinese Academy of Sciences, Beijing 100049, China; 3. Fujian Science & Technology Innovation Laboratory for Optoelectronic Information of China, Fuzhou 350108, China, 4. Intelligent Construction Automation Center, Kyungpook National University, Daegu 41566, Republic of Korea)

Abstract: Dy^{3+}-doped $SrGdGa_3O_7$ crystal was successfully grown through the Czochralski method and investigated in detail for its structural and optical features. Its crystallographic lattice parameters were optimized by Rietveld refinement based on XRD data. Polarized absorption spectra, polarized emission spectra, and fluorescence decay curves of Dy: $SrGdGa_3O_7$ crystal were analyzed. Absorption cross-sections at 452 nm corresponding to π- and σ-polarization were computed as 0.594×10^{-21} and 0.555×10^{-21} cm^2, respectively. Calculated effective J-O intensity parameters Ω_2, Ω_4, and Ω_6 were 5.495×10^{-20}, 1.476×10^{-20}, and 1.110×10^{-20} cm^2, respectively. J-O analysis and emission spectra show that transition $^4F_{9/2}\rightarrow{}^6H_{13/2}$ of Dy: $SrGdGa_3O_7$ crystal has the highest fluorescence branching ratio and fluorescence intensity under 452 nm excitation within the visible spectral region, the emission cross-sections of π- and σ-polarization were 1.84×10^{-21} and 2.49×10^{-21} cm^2 at the wavelength of 574 nm, respectively. The measured radiative lifetime and fluorescence decay time of the Dy^{3+}: $^4F_{9/2}$ level were 0.768 and 0.531 ms with a quantum efficiency of 69.1%. All these results reveal that Dy^{3+}: $SrGdGa_3O_7$ crystal is a promising material for yellow lasers pumped with blue laser diodes.

Key words: crystal growth; Dy^{3+}: $SrGdGa_3O_7$; optical properties; yellow emission

The yellow laser has promising applications, particularly in the field of medicine such as Freckle removal and the therapy of ophthalmic illness[1-2]. Among the existing solutions for achieving yellow laser output include solid-state gain medium-based summing frequency mixing, frequency doubling techniques, and optically pumped semiconductor lasers[3-5]. But these approaches have low output efficiency, complex system design, and higher expenses, which in turn limit the application of yellow lasers. Trivalent dysprosium (Dy^{3+}) ion possesses an abundant energy level structure that allows it to emit different colors of light in the visible region through 4f-4f energy level transitions[6]. As one of the few rare-earth ions capable of directly producing yellow emission (Dy^{3+}: $^4F_{9/2}\rightarrow{}^6H_{13/2}$), yellow lasers with Dy^{3+} doped crystals are promising for industrial, medical, and display applications, it has attracted much attentions. In 2012, the first InGaN LD pumped Dy: YAG crystal achieved yellow light laser operation with 150 mW output power[7]. Later, a continuous yellow laser output of 574 nm was obtained with InGaN LD-pumped Dy, Tb: $LiLuF_4$ crystal. The slope efficiency is only 13.4%, and the output power is 55 mW[8]. Furthermore, Dy: YAG crystal achieves laser operation at 582.7 nm with a single pulse energy of ~1.1 mJ at a repetition rate of 50 Hz[9]. The CW yellow laser output of Dy: YAG crystal has also progressed, achieving a maximum output power of 166.8 μW at a laser center wavelength of 582.5 nm[10]. Some studies of

Received date: 2023-02-06; **Revised date:** 2023-02-27; **Published online:** 2023-09-12
Foundation item: National Natural Science Foundation of China (51832007, 51872286); National Key Research and Development Program of China (2022YFB3605704); NSFC-Joint Funds for Regional Innovation and Development (U21A20508); Science and Technology Plan Leading Project of Fujian Province (2022H0043, 2020H0036); Fujian Science & Technology Innovation Laboratory for Optoelectronic Information of China (2021ZR204, 2020zz108); The 14th Five-year Plan Project of FJIRSM (E255KL0101); Science and Technology Service Network Initiative (2019T3006)
Biography: WANG Haidong (1997–), male, Master candidate. E-mail: wanghaidong@fjirsm.ac.cn
王海东(1997–), 男, 硕士研究生. E-mail: wanghaidong@fjirsm.ac.cn
Corresponding author: TU Chaoyang, professor. E-mail: tcy@fjirsm.ac.cn
涂朝阳, 研究员. E-mail: tcy@fjirsm.ac.cn

Dy co-doping with other ions have been carried out, such as Dy^{3+}/Y^{3+}: CaF_2[11], $Dy^{3+}/(Tb^{3+}, Eu^{3+})$: $Sr_3Gd(BO_3)_3$[12], Dy^{3+}/Tm^{3+}: $LiNbO_3$[13]. More importantly, to enhance the efficiency of the Dy^{3+} laser, it is indispensable to exploit suitable Dy^{3+}-doped matrix crystals.

$SrGdGa_3O_7$ crystal is a member of the Melilite $ABGa_3O_7$ (A = Ca, Ba, Sr, B = La, Gd) crystals, which belongs to the $P\bar{4}2_1m$ space group. The melting point is about 1600 ℃, and the congruent melting makes it suitable for crystal growth with the Czochralski method[14-16]. The ratio of the thermal expansion coefficient $SrGdGa_3O_7$ crystal in different polarization ($\alpha_a = 5.32\times10^{-6}$ /K, $\alpha_c = 5.365\times10^{-6}$ /K) is close to 1, which is beneficial for the growth of high-grade crystal and its applications in laser works[17]. $SrGdGa_3O_7$ is a disordered laser crystal, and the activating ion is affected by the crystal field where it is located, causing an inhomogeneous broadening of the spectra, which is beneficial to the semiconductor laser pumping efficiency. The wide emission spectrum makes $SrGdGa_3O_7$ a good crystal material for new ultrashort pulse lasers. Furthermore, $SrGdGa_3O_7$ crystal with lower phonon energy (~680 cm^{-1}) can meet the requirements for matrix crystals in both visible and mid-infrared regions[18]. At present, most of the studies on $SrGdGa_3O_7$ are focused on Nd^{3+}, Er^{3+}, and Tm^{3+}-activated crystals[15,17]. The visible and mid-infrared studies of Dy^{3+}-activated $SrGdGa_3O_7$ crystal have not yet been reported.

In this work, Dy^{3+}-doped $SrGdGa_3O_7$ crystal is successfully grown by the Czochralski method, and crystal structure, absorption, fluorescence, and fluorescence decay time of such crystal are investigated as a potential yellow laser gain medium.

1 Experimental

3% (in mass) Dy^{3+}-doped $SrGdGa_3O_7$ (Dy: SGGM for short) crystal was grown through the Czochralski method on (001) orientation. All chemical components were dried before weighing. The crystal was synthesized using $SrCO_3$ (AR), 99.999% purity Gd_2O_3, Ga_2O_3, and Dy_2O_3 raw materials according to the formula $SrGd_{0.97}Dy_{0.03}Ga_3O_7$. To compensate for the volatilization of Ga_2O_3 during the growth, additional 1% (in mass) Ga_2O_3 was added. The components were ground, mixed, and heated in a Corundum crucible at 1100 ℃ for 24 h. After cooling to ambient temperature, the mixtures were re-ground, pressed into bulks, and heated at 1200 ℃ for 48 h. An intermediate-frequency heater was used to melt the synthesized materials laid in the iridium crucible. During the crystal growth, the rotational rate was maintained at 8–12 r/min, and the pulling rate was 1–1.3 mm/h. When crystal growth completed, the crystal was cooled to ambient temperature at a rate of 15–30 K/h. As shown in Fig. 1, the as-grown Dy: SGGM crystal has dimensions of ϕ25 mm×40 mm. Effective concentration (C_{top}) for Dy^{3+} ions in Dy: SGGM crystal is 2.49% as measured by ICP-OES (Agilent 725 ES, USA), and segregation coefficient κ by calculation is 0.83.

The XRD (X-ray diffraction) pattern was obtained using a Rigaku MiniFlex-600 diffractometer and employing Cu Kα radiation (λ = 0.1540598 nm). The samples used for XRD measurements were powders obtained by grinding the crystals. A wafer with dimensions of 10 mm× 10 mm×1 mm is obtained by slicing and polishing for spectroscopic measurements. The rocking curve of the single crystal (002) plane was determined with an X-ray diffractometer (Germany-Bruker D8 Advance) with a scan step of 0.001°. Optical polarized absorption spectra were measured using a Perkin-Elmer UV-Vis-NIR spectrometer (Lambda-900) with a spectral resolution of 1 nm. Fluorescence spectra and fluorescence decay curves were measured with an Edinburgh FLS1000 photometer at continuous and pulsed Xe lamps, respectively, where the fluorescence spectra had a scanning slit width of 1 nm and the fluorescence decay curve had a slit width of 2 nm on the excitation side and 0.5 nm on the emission side. Experimental conditions were kept constant during the optical studies to obtain comparable results. All tests were carried out at ambient temperature.

2 Results and discussion

2.1 Crystal structure

Structure of the melilite $SrGdGa_3O_7$ crystal is shown in Fig. 2, the GaO_4 tetrahedron layer is in the *a-b* planes. There are two types of GaO_4 tetrahedra, one for Ga1 atoms and the other for Ga2 atoms, the symmetries are quartic symmetry and mirror symmetry. Gd^{3+} and Sr^{2+} are randomly distributed within the *a-b* layers in a ratio of 1∶1. The Jahn-Teller effect results in the asymmetry of Sr^{2+} and Gd^{3+} coordination environment, resulting in the disordered structure of the crystal and spectral inhomogeneously broadening[14]. In Dy: SGGM crystal, Dy^{3+} ions are equivalently substituted for Gd^{3+} ions, making rare-earth ion activation centers in the crystal with different coordination environments.

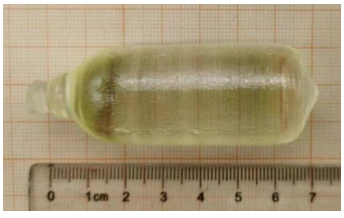

Fig. 1 Picture of as-grown Dy: SGGM single crystal

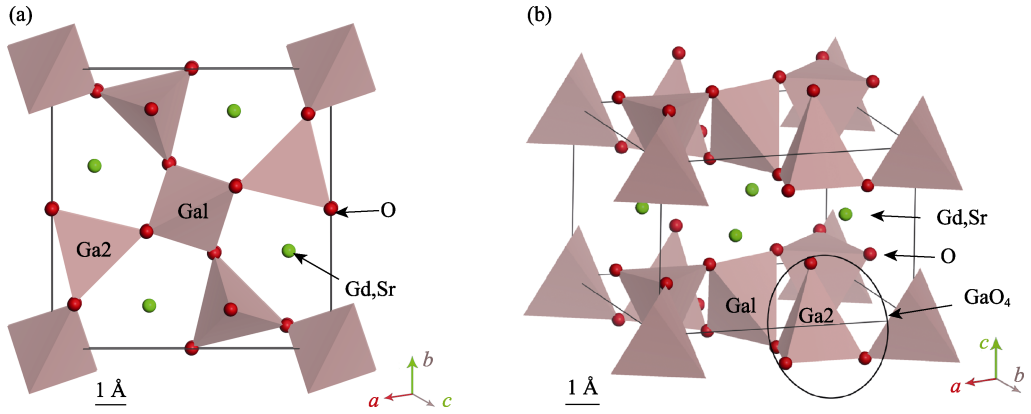

Fig. 2 Crystal structures of $SrGdGa_3O_7$ crystal
(a) Parallel to *c*-axis; (b) Vertical to *c*-axis

Fig. 3(a) displays XRD pattern of as-grown crystal. Diffraction peaks are quite matched to the standard JCPDF card of $SrGdGa_3O_7$ (50-1835). Rietveld refinement of XRD powder data from Dy: SGGM crystal was carried out by the GSAS-II program, and the result is illustrated in Fig. 3(b). The result is a reliable refinement with *R*-weighted profile residual (R_{wp})=12.456% and Goodness-of-fit indicator (χ^2)=1.35, where observed diffraction pattern agrees well with the calculated diffraction pattern, indicating that the Dy: SGGM crystal has a tetragonal phase and belongs to the space group of $P\bar{4}21m$. The doping of Dy^{3+} ions makes disorder of crystal structure increase and lattice constant becomes larger. The lattice parameters of Dy: SGGM crystal after refinement are shown in Table 1. Fig. 3(c) shows the rocking curve of the (002) plane of the Dy: SGGM crystal. 2θ of the (002) diffraction peak is 34.11°, and the peak shape is splitless and smoothly symmetric. The FWHM is 0.07°, reflecting the good crystalline quality of the grown crystal.

2.2 Absorption spectra and Judd-Ofelt analysis

$SrGdGa_3O_7$ is a uniaxial crystal, and polarized absorption spectra of Dy: SGGM crystal in the wavelength range of 315–1900 nm are illustrated in Fig. 4. In Fig. 4, mainly 13 absorption peaks centered at 323, 347, 361, 385, 425, 452, 471, 770, 789, 896, 1076, 1248, and 1758 nm, corresponding to the transitions from ground state $^6H_{15/2}$ to $^4G_{9/2}$+$^6P_{3/2}$+$^4M_{17/2}$, $^6P_{7/2}$+$^4I_{11/2}$, $^6P_{5/2}$+$^4D_{3/2}$+$^4M_{19/2}$, $^4F_{7/2}$+ $^4I_{13/2}$+$^4M_{21/2}$+$^4K_{17/2}$, $^4G_{11/2}$, $^4I_{15/2}$, $^4F_{9/2}$, $^6F_{3/2}$, $^6F_{5/2}$, $^6F_{7/2}$, $^6F_{9/2}$+$^6H_{7/2}$, $^6F_{11/2}$+$^6H_{9/2}$, $^6H_{11/2}$ level respectively are observed. In particular, the absorption peak corresponding to $^6H_{15/2}\rightarrow{}^4I_{15/2}$ transition is located at 452 nm, making it very suitable for laser diode (LD) pumping[19]. Absorption cross-section (σ_{abs}) of Dy: SGGM crystal is given by the equation:

$$\sigma_{abs} = \frac{\alpha}{N_c} \tag{1}$$

where N_c stands for lattice concentration, α represents the absorption coefficient. The lattice concentration of Dy^{3+} was calculated from ICP-OES measurements to be 1.498×10^{20} cm^{-3}. The FWHM of the absorption peaks at 452 nm for π- and σ-polarization are 10.4 and 11.8 nm, and absorption cross-sections (σ_{abs}) are 0.594×10^{-21} and 0.555×10^{-21} cm^2, respectively. Here σ_{abs} of Dy: SGGM crystal around 452 nm representing the $^4I_{15/2}$ level is smaller than those of other Dy^{3+}-doped crystals such as CeF_3[20], $CaYAlO_4$[21], $CaGdAlO_4$[22], and YAG[23]. However, Dy: SGGM crystal has a large FWHM compared with other crystals, which facilitates efficient diode pumping and is not easily affected by the temperature. The specific absorption spectral parameters are compared and listed in Table 2.

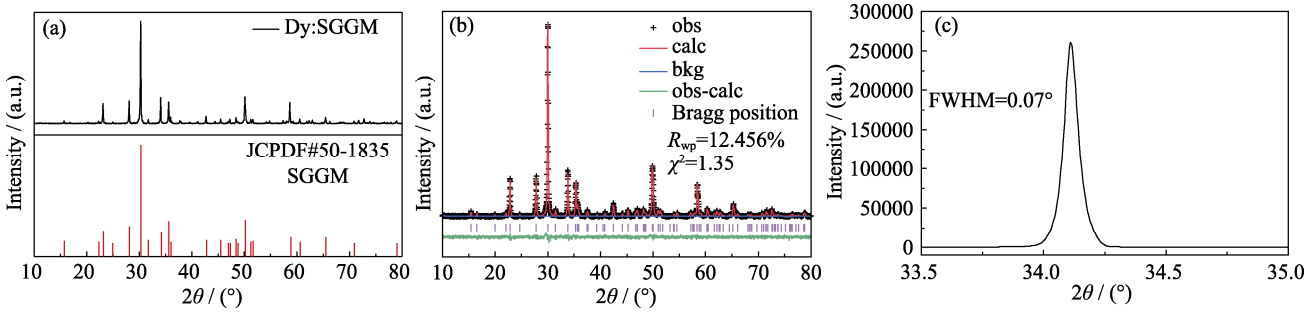

Fig. 3 Analysis of XRD results of Dy: SGGM crystal
(a) XRD pattern; (b) Rietveld refinement; (c) Rocking curve of (002) plane

Table 1 Comparison of structural parameters of Dy: SGGM crystal before and after Rietveld refinement

Parameter	Dy:SGGM	SGGM (PDF#50-1835)
a, b/nm	0.79741	0.79651
c/nm	0.52599	0.52368
V/nm^3	0.334460	0.33224
ρ/(g·cm^{-3})	5.670	5.658
Space group	$P\bar{4}2_1m$	
R_{wp}	12.456%	
χ^2	1.35	

The Judd-Ofelt theory is an effective method to probe the optical properties of the 4f-4f transitions of trivalent rare-earth ions[24-25]. Line strength $S_{calc}(J, J')$ of electric dipole transition and experimental line strength $S_{exp}(J, J')$ are calculated by following equations:

$$S_{calc}(J, J') = \sum_{t=2,4,6} \Omega_t |\langle S, L, J \| U^{(t)} \| S', L', J' \rangle|^2 \quad (2)$$

$$S_{exp}(J, J') = \frac{(2J+1)}{N_c} \frac{3hc}{8\pi^3 \bar{\lambda} e^2} \frac{9n}{(n^2+2)^2} \frac{\int OD(\lambda) d\lambda}{0.43l} \quad (3)$$

where $\left|\left\langle S, L, J \middle\| U^{(t)} \middle\| S', L', J' \right\rangle\right|^2$ represents the transition matrix element from J state to J' state. $\langle \| U^{(t)} \| \rangle$ is the squared reduced matrix elements. $OD(\lambda)$ represents a function of wavelength λ about optical density. h is Planck constant (6.626×10^{-27} erg·s), c represents the speed of light (2.998×10^{10} cm·s^{-1}), e is electron charge (4.803×10^{-10} esu), $\bar{\lambda}$ represents the average wavelength of absorption bands, l represents thickness of crystal, n represents index of refraction of crystal taken from Ref. [17].

RMS (root-mean-square) between the calculated and experimental intensities is described by:

$$RMS = \sqrt{\frac{\sum_{i=1}^{N} (S_{calc} - S_{exp})^2}{N-3}} \quad (4)$$

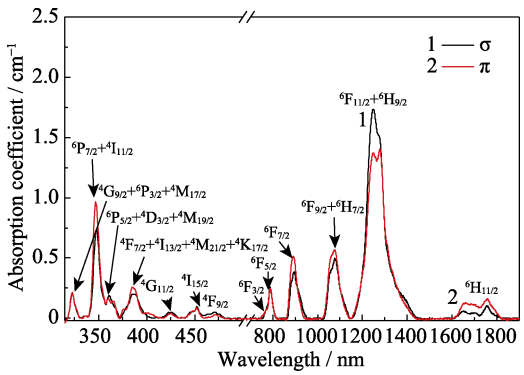

Fig. 4 Polarized absorption spectra of Dy: SGGM crystal

Table 2 Comparison of absorption spectral parameters of Dy^{3+}-doped crystals

Crystal	λ/nm	FWHM/ nm	σ_{abs}/ ($\times10^{-21}$, cm^2)	Ref.
Dy: CeF_3	450	9.4	0.61	[20]
Dy: $PbWO_4$	454	5.71	1.42	[26]
Dy: CNGS	453	10.2	1.2	[27]
Dy: $Sr_3Y(BO_3)_3$	450	8(π) 10(σ)	0.8(π) 0.6(σ)	[28]
Dy: $CaYAlO_4$	453	–	3.3(π) 2.1(σ)	[21]
Dy: $CaGdAlO_4$	452	2.5(π) 4.3(σ)	1.28(π) 2.43(σ)	[22]
Dy: YAG	447	1.9	2.3	[23]
Dy: SGGM	452	10.4(π) 11.8(σ)	0.594(π) 0.555(σ)	This work

where N is the number of absorption bands. Calculated RMS is 0.074×10^{-20} cm^2 (π-polarization) and 0.063×10^{-20} cm^2 (σ-polarization) in Dy: SGGM crystal, which suggests that calculated line strengths are relatively close to experimental line strengths. It also proves that the results are of good authenticity and credibility. Calculated and experimental line strengths of Dy: SGGM crystal are given in Table 3.

Table 4 lists three J-O intensity parameters of the Dy: SGGM crystal and comparison of them with some Dy^{3+}-doped materials. For polarization absorption, effective J-O intensity parameters are characterized by $\Omega_{t,eff}=(2\Omega_{t,\sigma} + \Omega_{t,\pi})/3$. The three effective J-O intensity parameters $\Omega_{t,eff}$ (t=2, 4, 6) are calculated to be 5.495×10^{-20}, 1.476×10^{-20}, 1.110×10^{-20} cm^2, respectively. In particular, Ω_2 reflects symmetry of lattice environment around rare-earth ions, which is strongly influenced by the coordination environment[29-30]. As shown in Table 4, the Ω_2 value in Dy: SGGM crystal is larger than that in Dy: $CaYAlO_4$[21], Dy: $Gd_3Ga_5O_{12}$[31], Dy: YAG[23]. The higher value of Ω_2, the lower lattice symmetry of rare-earth ion. $\Omega_{4,6}$ parameters reflect the rigidity and covalent of host material where rare-earth ions are located[32].

Spontaneous radiative rates (A_{ed}) of electric dipole transition and spontaneous radiation rates (A_{md}) of magnetic dipole transition are calculated by using following equations:

$$A_{total} = A_{md} + A_{ed} \quad (5)$$

$$A_{ed}(J, J') = \frac{64\pi^4 e^2}{3h(2J+1)\bar{\lambda}^3} \frac{n(n^2+2)^2}{9} S_{ed} \quad (6)$$

$$A_{md}(J, J') = \frac{64\pi^4 e^2 n^3}{3h(2J+1)\bar{\lambda}^3} S_{md} \quad (7)$$

As the variation of S_{md} is independent on host material, S_{md} values from Ref. [33] were used.

Table 3 Experimental and calculated line strengths in Dy:SGGM crystal

Transition $^6H_{15/2}\rightarrow$	π-polarization			σ-polarization		
	$\bar{\lambda}$/nm	$S_{exp}/(\times10^{-20}, cm^2)$	$S_{calc}/(\times10^{-20}, cm^2)$	$\bar{\lambda}$/nm	$S_{exp}/(\times10^{-20}, cm^2)$	$S_{calc}/(\times10^{-20}, cm^2)$
$^4G_{11/2}$	426	0.053	0.028	422	0.076	0.022
$^4I_{15/2}$	450	0.104	0.093	450	0.148	0.123
$^4F_{9/2}$	470	0.039	0.033	473	0.055	0.043
$^6F_{3/2}$	766	0.088	0.051	761	0.077	0.076
$^6F_{5/2}$	791	0.286	0.291	792	0.403	0.429
$^6F_{7/2}$	893	0.978	0.846	901	1.179	1.067
$^6H_{7/2}+^6F_{9/2}$	1074	1.631	1.672	1079	1.677	1.701
$^6H_{9/2}+^6F_{11/2}$	1266	6.670	6.660	1259	6.961	6.953
$^6H_{11/2}$	1693	0.970	1.078	1656	1.292	1.370
RMS/$(\times10^{-20}, cm^2)$		0.074			0.063	

Table 4 Comparison of J-O intensity parameters with other Dy^{3+}-doped materials

Crystal	$\Omega_2/(\times10^{-20}, cm^2)$	$\Omega_4/(\times10^{-20}, cm^2)$	$\Omega_6/(\times10^{-20}, cm^2)$	Ref.
Dy: $LiLuF_4$	2.04	0.91	1.09	[34]
Dy: YAG	1.49	0.94	3.20	[23]
Dy: $CaGdAlO_4$	1.80	1.00	0.50	[22]
Dy: $CaYAlO_4$	5.05	9.95	3.12	[21]
Dy: $Sr_3Y(BO_3)_3$	2.39	0.88	1.22	[28]
Dy: $LiNbO_3$	5.42	1.14	2.51	[35]
Dy: YSGG	0.13	0.73	1.06	[36]
Dy: GGG	0.17	2.66	2.57	[31]
Dy: SGGM	5.113 (π) 5.686 (σ) 5.495 (eff)	1.796 (π) 1.316 (σ) 1.476 (eff)	0.843 (π) 1.243 (σ) 1.110 (eff)	This work

Table 5 Calculated spontaneous emission probability, fluorescence branching ratio, and radiative lifetime of Dy: SGGM crystal

Transitions $^4F_{9/2}\rightarrow$	$\bar{\lambda}$/nm	A_{ed}/s^{-1}	A_{md}/s^{-1}	β	τ_r/ms
$^6F_{1/2}$	1364	0.094	0	7.220×10^{-5}	0.768
$^6F_{3/2}$	1270	0.066	0	5.055×10^{-5}	–
$^6F_{5/2}$	1157	9.804	0	7.526×10^{-3}	–
$^6F_{7/2}$	998	4.534	8.413	9.939×10^{-3}	–
$^6H_{5/2}$	921	3.577	0	2.746×10^{-3}	–
$^6H_{7/2}+^6F_{9/2}$	833	27.488	13.568	0.032	–
$^6H_{9/2}+^6F_{11/2}$	756	45.544	81.59	0.098	–
$^6H_{11/2}$	665	86.029	17.474	0.079	–
$^6H_{13/2}$	574	841.755	0	0.646	–
$^6H_{15/2}$	481	162.738	0	0.125	–

Radiative branching ratio β and radiative lifetime τ_r are described as:

$$\beta(J,J') = \frac{A(J,J')}{\sum_{J'} A(J,J')} \tag{8}$$

$$\tau_r = \frac{1}{\sum_{J'} A(J,J')} \tag{9}$$

The spontaneous transition rate A_{total} ($A_{total} = A_{md} + A_{ed}$), fluorescence branching ratio β, and radiation lifetime τ_r of Dy: $^4F_{9/2}$ level in Dy: SGGM crystal are listed in Table 5. Calculated β for transition $^4F_{9/2}\rightarrow{}^6H_{13/2}$ is 0.646, indicating that Dy: SGGM crystal has better yellow light emitting capability.

2.3 Yellow fluorescence spectra and fluorescence lifetime

Emission spectra of Dy: SGGM crystal in 450–800 nm wavelength range are measured upon 452 nm excitation, and obtained spectra are presented in Fig. 5. Transitions from $^4F_{9/2}$ to $^6H_{15/2}$, $^6H_{13/2}$, $^6H_{11/2}$, and $^6H_{9/2}$ + $^6F_{11/2}$ are observed, corresponding to wavelengths of 476, 574, 660, and 754 nm, respectively. Yellow emission peak at 574 nm has the highest fluorescence intensity, which is in general consistent with calculated fluorescence branching ratio.

The excited level's emission cross-section (σ_{em}) in the crystal is one of the most important factors, which affects the output power and light conversion efficiency of the lasers. Based on the absorption spectra, the emission cross-section was obtained by using the Füchtbauere-Ladenburg (F-L) equation[37]:

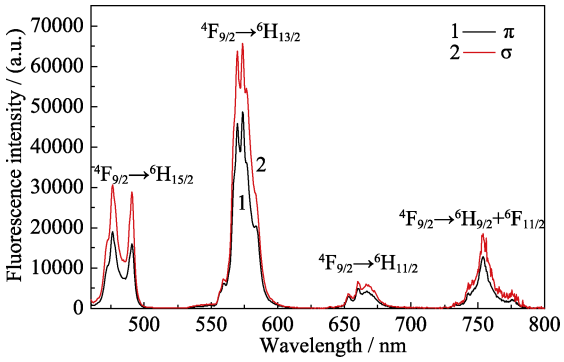

Fig. 5 Polarized emission spectra of Dy:SGGM crystal

$$\sigma_{em}(\lambda)=\frac{\lambda^5 I(\lambda)\beta}{8\pi cn^2\tau_r\int I(\lambda)\lambda d\lambda} \quad (10)$$

where $I(\lambda)$ is experimental fluorescence intensity as a function of wavelength λ, n means refractive index, c represents the speed of light, β is fluorescence branching ratio, τ_r stand for radiative decay time of an excited state.

For anisotropic uniaxial crystals, emission cross-section in the π- and σ- polarization needs to be calculated separately, and here the emission cross-section is expressed as:

$$\sigma_{em}(\lambda)=\frac{3\lambda^5 I_{\sigma,\pi}(\lambda)\beta}{8\pi cn^2\tau_r\int[2I_\sigma(\lambda)+I_\pi(\lambda)]\lambda d\lambda} \quad (11)$$

Emission cross-section for the σ- and π- polarizations at 574 nm in the Dy: SGGM crystal are estimated to be 1.84×10^{-21} and 2.49×10^{-21} cm^2. As presented in Table 6, the values of σ_{em} is higher than those of Dy: $CaGdAlO_4$[22], Dy: $Sr_3Y(BO_3)_3$[28], and Dy: CNGS[27], but smaller than those of Dy: $CaYAlO_4$[21] and Dy: GGG[31]. Furthermore, Dy: SGGM crystal has a broadband emission at around 574 nm for which the FWHM is 15.6 nm (π-polarisation) and 16.2 nm (σ-polarisation). It is beneficial to acquire tunable yellow laser and ultrashort pulsed laser outputs in the corresponding wavelength bands.

Chromaticity coordinates can be used to assess the color of overall emission in the visible range. For π- and σ-polarizations in Dy: SGGM crystal under 452 nm excitation, it can be calculated by CIE 1931 program as (x_1=0.4075, y_1=0.4527) and (x_2=0.3986, y_2=0.4431) respectively. The chromaticity coordinates belong to the yellow wavelength range, and correlated color temperature (CCT) can be computed according to the equation[38]:

$$CCT=-449N^3+3525N^2-6823.3N+5520.33 \quad (12)$$

where $N=(x-x_e)/(y-y_e)$, chromaticity epicentre is (x_e=0.3320, y_e=0.1858). For π- and σ-polarizations, CCT value is calculated to be 3862 and 3982 K, respectively. Calculated chromaticity coordinates fall within the yellow light range, as illustrated in Fig. 6, which suggests the potential of Dy: SGGM crystal for yellow light applications.

Fig. 7 displays the fluorescence decay curve of Dy: $^4F_{9/2}$ level at 574 nm excited under 452 nm wavelength. The measured curve follows double-exponential functions, and the fluorescence lifetime (τ_f) of Dy^{3+}:$^4F_{9/2}$ level calculated is 0.531 ms. Besides, the radiative lifetime of

Table 6 Comparative spectral features of some Dy^{3+}-doped crystals

Crystals	$\bar{\lambda}$/nm	FWHM/nm	σ_{em}/(×10^{-21}, cm^2)	τ_r/ms	τ_f/ms	η/%	Ref.
Dy:$LiNbO_3$	575	–	3.2 (π) 0.3 (σ)	0.292	0.268	91.8	[35]
Dy:YAG	583	–	2.09	1.02	0.4	39.2	[23]
Dy: $CaYAlO_4$	580	–	2.8 (π) 3.6 (σ)	0.485	0.262	54.0	[21]
Dy:$CaGdAlO_4$	578	13(π) 14 (σ)	0.55 (π) 0.51 (σ)	0.501	0.222	44.3	[22]
Dy:$Sr_3Y(BO_3)_3$	576	16 (σ) 17 (π)	1.0 (σ) 1.2 (π)	1.45	0.820	56.6	[28]
Dy: CNGS	572	16.3 (σ) 15.8 (π)	1.35 (σ) 1.89 (π)	1.22	0.293	26.5	[27]
Dy:GGG	581	–	2.62	1.107	0.79	71.4	[31]
Dy:SGGM	574	15.6(π) 16.2(σ)	1.84 (π) 2.49 (σ)	0.768	0.531	69.1	This work

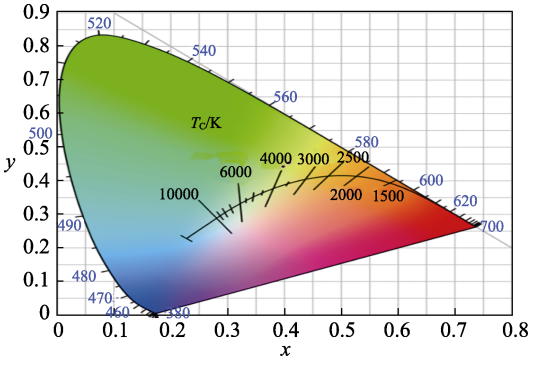

Fig. 6 Chromaticity coordinates of Dy: SGGM crystal under 452 nm excitation

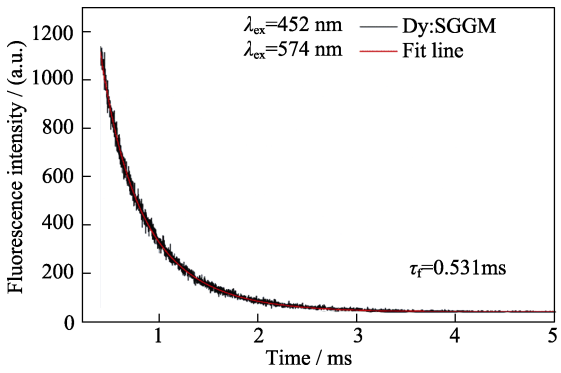

Fig. 7 Fluorescence decay curve of Dy:SGGM crystal

Dy^{3+}:$^4F_{9/2}$ multiplet obtained from calculations of J-O theory was 0.768 ms. The cross-relaxation of Dy^{3+} ions as the main factor of the short fluorescence lifetime of $^4F_{9/2}$ multiplet can be improved by optimizing Dy^{3+} ion concentration[39-40]. The quantum efficiency $(\eta = \tau_f / \tau_r)$ of Dy^{3+}:$^4F_{9/2}$ multiplet is 69.1%, which is larger than that of Dy: $CaYAlO_4$ (54.0%)[21], but smaller than those of Dy: $LiNbO_3$ (91.8%)[35] and Dy: GGG (71.4%)[31]. All these features indicate Dy: SGGM crystal as a promising candidate for yellow laser.

3 Conclusions

In summary, Dy: SGGM crystal with dimensions of ϕ25 mm×40 mm was successfully grown by the CZ method. Lattice parameters of Dy: SGGM crystal were optimized with Rietveld refinement based on XRD data. The polarized absorption spectra, polarized emission spectra, and fluorescence decay curves of the Dy: SGGM crystal were studied in detail. The absorption peak at the Dy: $^4I_{15/2}$ level is around 452 nm, and its absorption cross-section for π- and σ- polarization is 0.594×10^{-21} and 0.555×10^{-20} cm^2, respectively. The FWHM of σ_{abs} is 10.4 nm (π-polarization) and 11.8 nm (σ-polarization) accordingly, which is particularly favorable for blue LD pumping. Three effective J-O intensity parameters were calculated to be: $\Omega_{2,eff}$=5.495×10^{-20} cm^2, $\Omega_{4,eff}$=1.476×10^{-20} cm^2, and $\Omega_{6,eff}$=1.110×10^{-20} cm^2. Calculated emission cross-sections at 574 nm for π- and σ-polarization were 1.84×10^{-21} and 2.49×10^{-21} cm^2 by the FL method, and its FWHM was measured to be 15.6 nm (π-polarization) and 16.2 nm (σ-polarization). Fluorescence and radiation lifetime of Dy: $^4F_{9/2}$ level were 0.531 and 0.768 ms respectively with a quantum efficiency of 69.1%. All results show that Dy: SGGM crystal has a high potential to achieve a 574 nm yellow laser.

References:

[1] LEE H I, LIM Y Y, KIM B J, *et al.* Clinicopathologic efficacy of copper bromide plus/yellow laser (578 nm with 511 nm) for treatment of melasma in Asian patients. *Dermatologic Surgery*, 2010, **36(6):** 885.

[2] KIM J Y, PARK H S, KIM S Y. Short-term efficacy of subthreshold micropulse yellow laser (577-nm) photocoagulation for chronic central serous chorioretinopathy. *Graefe's Archive for Clinical and Experimental Ophthalmology*, 2015, **253(12):** 2129.

[3] SINHA S, LANGROCK C, DIGONNET M J, *et al.* Efficient yellow-light generation by frequency doubling a narrow-linewidth 1150 nm ytterbium fiber oscillator. *Optics Letters*, 2006, **31(3):** 347.

[4] CHEN Y F, TSAI S W. Diode-pumped Q-switched Nd:YVO_4 yellow laser with intracavity sum-frequency mixing. *Optics Letters*, 2002, **27(6):** 397.

[5] VILERA M, CHRISTENSEN M, HANSEN A K, *et al.* 2.7 W diffraction-limited yellow lasers by efficient frequency doubling of high-brightness tapered diode lasers. *Optics Communications*, 2019, **435:** 145.

[6] XU J, XU X D, HOU W T, *et al.* Research progress of rare-earth doped laser crystals in visible region. *Journal of Inorganic Materials*, 2019, **34(6):** 573.

[7] BOWMAN S R, O'CONNOR S, CONDON N J. Diode pumped yellow dysprosium lasers. *Optics Express*, 2012, **20(12):** 12906.

[8] BOLOGNESI G, PARISI D, CALONICO D, *et al.* Yellow laser performance of Dy^{3+} in co-doped Dy,Tb:$LiLuF_4$. *Optical Letter*, 2014, **39(23):** 6628.

[9] JU Q, SHEN H, YAO W M, *et al.* Laser diode pumped Dy: YAG yellow laser. *Chinese Journal of Lasers*, 2017, **44(4):** 0401004.

[10] YANG J X, LI W, WANG Y, *et al.* Spectroscopic and yellow Laser features of Dy^{3+}: $Y_3Al_5O_{12}$ single crystals. *Journal of Inorganic Materials*, 2023, **38(3):** 350.

[11] GAO X q, FANG G y, WANG Y, *et al.* Visible and mid-infrared spectral performances of Dy^{3+}: CaF_2 and Dy^{3+}/Y^{3+}: CaF_2 crystals. *Journal of Alloys and Compounds*, 2021, **856:** 158083.

[12] FANG G Y, WANG Y, YOU Z Y, *et al.* Crystal growth, spectral properties and energy transfer mechanisms of $Sr_3Gd(BO_3)_3$:Dy^{3+}/RE^{3+} (RE=Tb, Eu) crystals. *Chinese Journal of Luminescence*, 2022, **43(11):** 1721.

[13] LONG S W, MA D C, ZHU Y Z, *et al.* Temperature dependence of white light emission and energy transfer in Dy^{3+} and Tm^{3+} co-doped $LiNbO_3$ single crystals. *Journal of Luminescence*, 2017, **192:** 728.

[14] ZHANG Y Y, YIN X, YU H H, *et al.* Growth and piezoelectric properties of melilite ABC_3O_7 crystals. *Crystal Growth & Design*, 2011, **12(2):** 622.

[15] XIA H P, FENG J H, JI Y X, *et al.* 2.7 μm emission properties of $Er^{3+}/Yb^{3+}/Eu^{3+}$: $SrGdGa_3O_7$ and $Er^{3+}/Yb^{3+}/Ho^{3+}$: $SrGdGa_3O_7$ crystals. *Journal of Quantitative Spectroscopy and Radiative Transfer* 2016, **173:** 7.

[16] WANG Y, SUN C T, TU C Y, *et al.* Melilite-type oxide $SrGdGa_3O_7$: bulk crystal growth and theoretical studies upon both chemical bonding theory of single crystal growth and DFT methods. *Crystal Growth & Design*, 2018, **18(3):** 1598.

[17] ZHANG Y Y, ZHANG H J, YU H H, *et al.* Synthesis, growth, and characterization of Nd-doped $SrGdGa_3O_7$ crystal. *Journal of Applied Physics*, 2010, **108(6):** 063534.

[18] XIA H P, FENG J H, WANG Y, *et al.* Evaluation of spectroscopic properties of $Er^{3+}/Yb^{3+}/Pr^{3+}$: $SrGdGa_3O_7$ crystal for use in mid-infrared lasers. *Science Reports*, 2015, **5:** 13988.

[19] KRÄNKEL C, MARZAHL D-T, MOGLIA F, *et al.* Out of the blue: semiconductor laser pumped visible rare-earth doped lasers. *Laser & Photonics Reviews*, 2016, **10(4):** 548.

[20] YANG Y L, ZHANG L H, LI S M, *et al.* Crystal growth and 570 nm emission of Dy^{3+} doped CeF_3 single crystal. *Journal of Luminescence*, 2019, **215:** 166707.

[21] CHEN H, LOISEAU P, AKA G. Optical properties of Dy^{3+}-doped $CaYAlO_4$ crystal. *Journal of Luminescence*, 2018, **199:** 509.

[22] XU X D, HU Z W, LI R J, *et al.* Optical spectroscopy of Dy^{3+}-doped $CaGdAlO_4$ single crystal for potential use in solid-state yellow lasers. *Optical Materials*, 2017, **66:** 469.

[23] PAN Y X, ZHOU S D, LI D Z, *et al.* Growth and optical properties of Dy:$Y_3Al_5O_{12}$ crystal. *Physica B: Condensed Matter*, 2018, **530:** 317.

[24] OFELT G S. Intensities of crystal spectra of rare-earth ions. *The Journal of Chemical Physics*, 1962, **37(3):** 511.

[25] JUDD B R. Optical absorption intensities of rare-earth ions. *Physical Review*, 1962, **127(3):** 750.

[26] SHI Z L, LI Q, XUE Y Y, *et al.* Spectroscopic characterizations of Dy: $PbWO_4$ crystal. *Journal of Luminescence*, 2021, **236:** 118130.
[27] CHEN X T, HUANG Y S, YUAN F F, *et al.* A novel yellow laser candidate: Dy^{3+} doped $Ca_3NbGa_3Si_2O_{14}$ crystal. *Journal of Crystal Growth*, 2021, **564:** 126114.
[28] JIANG T H, CHEN Y J, GONG X H, *et al.* Spectroscopic properties of Dy^{3+}-doped $Sr_3Y(BO_3)_3$ crystal. *Optical Materials*, 2019, **91:** 171.
[29] ZEKRI M, HERRMANN A, TURKI R, *et al.* Experimental and theoretical studies of Dy^{3+} doped alkaline earth aluminosilicate glasses. *Journal of Luminescence*, 2019, **212:** 354.
[30] VIJAYA BABU K, COLE S. Luminescence properties of Dy^{3+}-doped alkali lead alumino borosilicate glasses. *Ceramics International*, 2018, **44(8):** 9080.
[31] WANG Y, YOU Z Y, LI J F, *et al.* Optical properties of Dy^{3+} ion in GGG laser crystal. *Journal of Physics D: Applied Physics*, 2010, **43(7):** 075402.
[32] POONAM, SHIVANI, ANU, *et al.* Judd-Ofelt parameterization and luminescence characterization of Dy^{3+} doped oxyfluoride lithium zinc borosilicate glasses for lasers and w-LEDs. *Journal of Non-Crystalline Solids*, 2020, **544:** 120187.
[33] RUKMINI E, JAYASANKAR C K. Spectroscopic investigations of Dy^{3+} ions in borosulphate glasses. *Physica B: Condensed Matter*, 1997, **240:** 273.
[34] BIGOTTA S, TONELLI M, CAVALLI E, *et al.* Optical spectra of Dy^{3+} in KY_3F_{10} and $LiLuF_4$ crystalline fibers. *Journal of Luminescence*, 2010, **130(1):** 13.
[35] RYBA-ROMANOWSKI W, DOMINIAK-DZIK G, SOLARZ P, *et al.* Transition intensities and excited state relaxation dynamics of Dy^{3+} in crystals and glasses: a comparative study. *Optical Materials*, 2009, **31(11):** 1547.
[36] SARDAR D K, BRADLEY W M, YOW R M, *et al.* Optical transitions and absorption intensities of Dy^{3+} ($4f^9$) in YSGG laser host. *Journal of Luminescence*, 2004, **106(3):** 195.
[37] AULL B, JENSSEN H. Vibronic interactions in Nd:YAG resulting in nonreciprocity of absorption and stimulated emission cross sections. *IEEE Journal of Quantum Electronics*, 1982, **18(5):** 925.
[38] MCCAMY C S. Correlated color temperature as an explicit function of chromaticity coordinates. *Color Research & Application*, 1992, **17:** 12590.
[39] LIU Y Y, TU C Y. Research progress on Dy-activated crystals to realize yellow emission in one step *via* commercial blue LD pumping. *Progress in Solid State Chemistry*, 2022, **67:** 100368.
[40] LIU Y, PAN F, TU C, *et al.* Structure, first-principles calculations and yellow spectral properties of Dy^{3+}: $CaLaGa_3O_7$ single crystal. *Journal of Luminescence*, 2021, **236:** 118122.

Dy^{3+}掺杂 $SrGdGa_3O_7$ 晶体的晶体生长, 结构、光学和可见光荧光特性

王海东[1,2,3], 王 燕[1,3], 朱昭捷[1,3], 李坚富[1,3],
LAKSHMINARAYANA Gandham[4], 涂朝阳[1,3]

(1. 中国科学院 福建物质结构研究所, 福州 350002; 2. 中国科学院大学, 北京 100049; 3. 中国福建光电信息科学与技术创新实验室(闽都创新实验室), 福州 350108; 4. 韩国庆北国立大学智能建筑自动化中心, 大邱 41566, 韩国)

摘 要: 采用 Chzochralski 方法成功生长了 Dy^{3+}掺杂的 $SrGdGa_3O_7$ 晶体, 并对其结构和光学特性进行了详细研究。基于 XRD 数据, 采用 Rietveld 法优化了晶体的晶格参数。分析了 Dy: $SrGdGa_3O_7$ 晶体的偏振吸收谱、偏振发射谱和荧光衰减曲线。在 452 nm 处, π 偏振和 σ 偏振对应的吸收截面分别为 0.594×10^{-21} 和 0.555×10^{-21} cm^2。计算得到的有效 J-O 强度参数 Ω_2、Ω_4 和 Ω_6 分别为 5.495×10^{-20}、1.476×10^{-20} 和 1.110×10^{-20} cm^2。J-O 理论分析和荧光光谱表明: 在 452 nm 激发下, Dy: $SrGdGa_3O_7$ 晶体 $^4F_{9/2}\rightarrow{}^6H_{13/2}$ 跃迁在可见光波段具有最高的荧光分支比和荧光强度, 在 574 nm 处的 π 和 σ 偏振发射截面分别为 1.84×10^{-21} 和 2.49×10^{-21} cm^2。Dy^{3+}: $^4F_{9/2}$ 能级的辐射寿命和荧光寿命分别为 0.768 和 0.531 ms, 量子效率为 69.1%。研究结果表明: Dy^{3+}: $SrGdGa_3O_7$ 晶体是一种潜在的可用于蓝光 LD 泵浦实现黄激光的材料。

关 键 词: 晶体生长; Dy^{3+}: $SrGdGa_3O_7$; 光学性能; 黄光发射

中图分类号: TN244 **文献标志码:** A